SoH-Aware Reconfiguration in Battery Packs

Liang He, *Member, IEEE*, Zhe Yang, *Member, IEEE*, Yu Gu, *Member, IEEE*, Cong Liu, *Member, IEEE*, Tian He, *Senior Member, IEEE*, and Kang G. Shin, *Life Fellow, IEEE*

***Abstract*—Cell imbalance, a notorious but widely found issue, degrades the performance and reliability of large battery packs, especially for cells connected in series where their overall capacity delivery is dominated by the weakest cell. In this paper, we exploit the emerging reconfigurable battery packs to mitigate the cell imbalance via the joint consideration of system reconfigurability and State-of-Health (SoH) of cells. Via empirical measurements and validation, we observe that more capacity can be delivered when cells with similar SoH are connected in series during discharging. Based on this observation, we propose two SoH-aware reconfiguration algorithms focusing on fully and partially reconfigurable battery packs, and prove their (near) optimality in capacity delivery. We evaluate the proposed reconfiguration algorithms analytically, experimentally, and via emulations, showing 10%–60% improvement in capacity delivery when compared with SoH-oblivious approaches, especially when facing severe cell imbalance.**

***Index Terms*—Reconfigurable battery packs, state-of-health, cell imbalance, cell graph.**

I. Introduction

LARGE battery packs, with their ability to support loads with high energy/power requirements, are widely used in systems such as electric vehicles and micro grids. The increased battery pack scale, however, incurs new challenges on their management. Reconfigurable battery packs have recently been investigated to address these challenges [2]–[4], with which the connectivity among cells can be actively altered according to load requirements and system states. Significant efforts have been devoted in this direction, such as achieving high reconfigurability with low system complexity [5], matching the supplied and desired voltages in real time [6], trading off between cycle efficiency and capacity utilization of the battery pack [7], and charging cells to their full capacity [8].

Manuscript received June 3, 2016; revised October 18, 2016; accepted November 27, 2016. Date of publication December 14, 2016; date of current version June 19, 2018. This work was supported in part by the NSF under Grant CNS-1329702, Grant CNS-1446117, and Grant CNS-1503590, and in part by the State Key Laboratory of Industrial Control Technology under Grant ICT1600206 and Grant NSFC-61402372. An early version of this work is published at ICCPS'15 [1]. Paper no. TSG-00747-2016. *(Corresponding author: Zhe Yang.)*

L. He is with the University of Colorado Denver, Denver, CO 80204 USA.

K. G. Shin is with the University of Michigan, Ann Arbor, MI 48109 USA.

Z. Yang is with Northwestern Polytechnical University, Xi'an 710072, China (e-mail: zyang@nwpu.edu.cn).

Y. Gu is with IBM Watson Health, Austin, TX 78613 USA.

C. Liu is with the University of Texas at Dallas, Richardson, TX 75081 USA.

T. He is with the University of Minnesota, Minneapolis, MN 48109 USA.

Color versions of one or more of the figures in this paper are available online at http://ieeexplore.ieee.org.

Digital Object Identifier 10.1109/TSG.2016.2639445

Cell imbalance is another crucial challenge in large battery packs [5], [9]. Due to uncontrollable factors such as active material dissolution and operating temperature, the capabilities of individual cells within a pack to accept and provide charge (termed as *State-of-Health* (SoH) of cells) diverge over usage. The unbalanced cells degrade the pack's performance; particularly, during discharging, the weakest cell (i.e., the cell with the lowest SoH) in a cell string (i.e., a set of series connected cells) dominates the string's capacity. Discharging the string beyond this limit causes severe heating issue, risking system safety.

In this paper, we propose the joint exploration of system reconfiguration and cells' SoH to mitigate cell imbalance. Our empirical measurements reveal enhanced capacity delivery by connecting cells with similar SoH in series, i.e., making cells with similar SoH share the same string, especially when facing severe cell imbalance. This observation inspires us the design of `SHARE-Full` and `SHARE-Partial`, two SoH-Aware REconfiguration algorithms to determine a proper system configuration based on cells' SoH, focusing on fully and partially reconfigurable battery packs, respectively. The contributions of this paper include:

- Revealing that forming cell strings with cells of similar SoH improves their capacity delivery (Section III);
- Design of `SHARE-Full` and `SHARE-Partial`, two SoH-aware reconfiguration algorithms for fully and partially reconfigurable battery packs, respectively (Section IV);
- Performance analysis of the design (Section V);
- Evaluations using experiments and emulations (Section VI).

II. Related Work

Recently, reconfigurable battery packs have be attracting increasing attentions from both academia and industry [4], [5], [10], [11], because of their advantages in higher efficiency [2], [6]–[8] and stronger robustness [9]. Existing studies on reconfigurable battery packs can be classified into two categories: *offering* reconfigurability and *exploiting* reconfigurability.

• **Physical Design of Reconfigurable Battery Packs.** The system reconfigurability is achieved by adding switches into the battery pack and thus increases system complexity. Much research effort has been devoted to achieve high reconfigurability with low system complexity [12]. Kim *et al.* [3] proposed a reconfigurable battery pack design in which each cell is equipped with two switches — one for connecting the

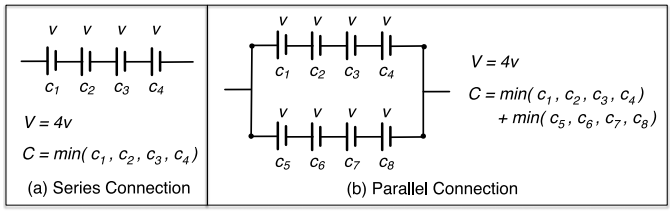

Fig. 1. Series and parallel connection of cells.

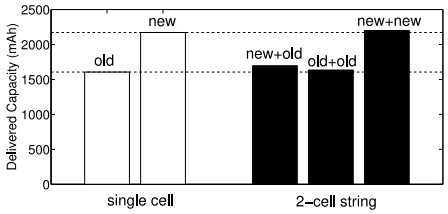

Fig. 2. Weak cell dominates string capacity.

cell to the load and the other for skipping the cell. With this design, any subset of cells can be sequentially connected in series, but no parallel strings can be formed. A reconfigurable battery pack where three switches are equipped for individual cells is designed in [13]. Increasing the per-cell switches to six, a reconfigurable battery pack supporting multiple outputs was proposed in [5].

• **Reconfiguration-Assisted Optimization.** The other category of existing work on reconfigurable battery packs focuses on exploitation of the offered reconfigurability to improve the battery performance. A reconfigurable battery string is proposed in [14] to adjust the supplied voltage to the load required level. The additional consideration on minimizing the discharge current of individual battery cells is incorporated into the reconfiguration design in [6]. Utilizing the battery pack reconfigurability to assist in charging cells to their fully capacity has been investigated in [8]. A reconfigurable battery pack consisting of various kinds of cells is explored in [10]. Molenaar exploited the battery reconfiguration to achieve fast charging of vehicles in [15].

Our work here falls in the second category to exploit the offered reconfigurability. However, different from these existing studies, in this paper, we explore the joint utilization of battery pack reconfigurability and cells' SoH to mitigate the cell imbalance during discharging.

III. Preliminaries and Motivations

A. Series and Parallel Connection of Cells

In general, cells in a battery pack can be connected in series or in parallel. The series connection of cells (i.e., cell string) increases the supplied voltage but its deliverable capacity is dominated by the weakest cell. On the other hand, connecting cells in parallel does not increase the supplied voltage but achieves higher deliverable capacity. For example, when connecting four cells in series as shown in Fig. 1(a), the supplied voltage is the sum of the four cells, while the deliverable capacity is dominated by the cell with the least capacity. On the other hand, connecting multiple cell strings in parallel achieves a capacity that is the sum of their respective deliverable capacities (Fig. 1(b)). This fact is further ensured by the common practice to add diode to each string to mitigate the imbalance among multiple cell strings, as will be explained in Section III-D.

The fact that *the weakest cell of a cell string dominates its capacity delivery* is the fundamental property that inspires this work. To demonstrate this, we collect a set of measurements with four *off-the-shelf* 2, 300mAh cells — two of them have been in use over one year (and thus are weaker) and the other two are new (and thus are stronger). Fig. 2 plots the collected results when discharging these cells with 2, 300mA current. The new cells deliver 2, 171mAh capacity on average, while the old cells deliver only 1, 606mAh. Then we form three 2-cell strings (i.e., *new-and-old*, *old-and-old*, and *new-and-new*) and again discharge them with 2, 300mA current. A clear observation is that the *new-and-old* string delivers similar capacity as the old cells, validating the string capacity is dominated by the weakest cell.

B. Cell Imbalance and State-of-Health

The strengths of cells in a battery pack tend to differ over usage due to many uncontrollable factors, commonly referred to as *cell imbalance*. Cell imbalance degrades battery pack performance, especially for cells connected in series where the string strength is dominated by the weakest cell.

To demonstrate the cell imbalance, we disassembled a 6-cell Li-ion battery pack used in a laptop and discharged them individually with a current of 2, 300 mA until the 2.8 V cut-off voltage[1] is reached. The cells' delivered capacities are plotted in Fig. 3(a), with a maximum and minimum of 1, 482 mAh and 1, 234 mAh, respectively, indicating a difference as large as 20%. Also, traditional wisdom shows that the cell imbalance in battery packs increases over time and usage [16]. To examine this exaggerated cell imbalance, Fig. 3(b) shows the capacity delivery of another set of 6 Li-ion cells when (i) they were newly purchased in May 2015 and (ii) measured again with the same discharge profile at May 2016. These cells have close capacity delivery when new (i.e., with differences below 20mAh), but show high diversity after 1 year usage.

The state-of-health (SoH) of cells quantifies their strength, whose variance indicates the cell imbalance degree in a pack. Specifically, focusing on the capacity fading of the batteries, SoH is defined as

$$SoH = Q_{\text{full}}/Q_{\text{rated}} \times 100\%, \tag{1}$$

where Q_{full} is the capacity delivered from a cell when discharging it from fully charged to fully discharged states [17], and Q_{rated} is the cell's originally rated capacity. Taking the new cell as of 100% SoH, a fully charged 2, 300mAh cell with 80% SoH can only deliver a capacity of about $2,300 \times 80\% = 1,840$mAh. The estimation of cell SoH has been studied extensively [17]–[20] and is supported by many commercial battery management systems and chips, e.g., the MAX17050 fuel gauge chip.

[1]The voltage defines the empty state of cells.

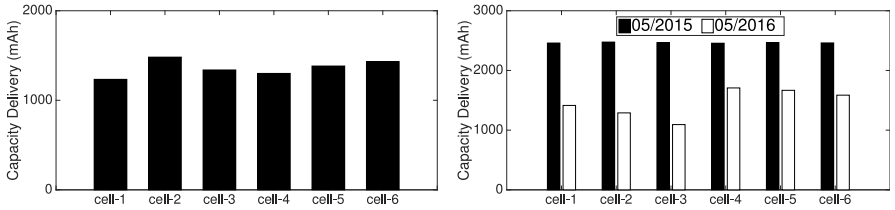

(a) Capacity of cells in a laptop battery. **(b)** Capacity of cells in 2015 and 2016.

Fig. 3. Measurement results on cell imbalance.

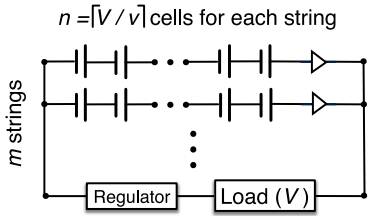

Fig. 4. System model.

C. Reconfigurable Battery Packs

The theme of this paper is to mitigate the cell imbalance with reconfigurable battery packs, which allow to jointly determine the battery pack configuration based on cells' SoH and the load requirements (i.e., SoH-aware (re)configuration), thus improving the battery pack's capacity delivery. Specifically, a reconfigurable battery pack can be represented by a weighted directed graph $\mathcal{G} = \{\mathcal{V}, \mathcal{E}, \mathcal{W}\}$ [6]:

- each vertex in $\mathcal{V}$ represents a cell in the system, and thus $|\mathcal{V}| = N$ where N is the number of cells in the battery pack;
- $\mathcal{E}$ reflects how these cells can be connected to each other and thus captures the system reconfigurability: an edge $v_i \rightarrow v_j \in \mathcal{E}$ if and only if the two corresponding cells can be directly connected in the battery pack;
- the weight set $\mathcal{W}$ on the vertices captures cells' SoH.[2]

D. System Model and Application Scenario

We consider the system model shown in Fig. 4. The battery pack consists of N cells each with nominal capacity c and voltage v. A voltage output of V is required by the load, meaning $n = \lceil \frac{V}{v} \rceil$ cells are required to form a series string. This way, a total number of m ($m \leq N/n$) such strings can be formed and connected in parallel to supply the load. Cell voltage deviates from the nominal voltage v during discharging. As a result, *(i)* a diode is attached to each string to avoid the reverse charging caused by the voltage difference among cell strings; *(ii)* a voltage regulator is used to provide a stable voltage to the load. These are also the common approach to handle cell voltage changes in practice [21].

After charging, the battery pack is reconfigured based on cells' SoH, and then used to support the load (i.e., discharging). A real-life example of this scenario is to reconfigure the battery pack after charging an electric vehicle over night at home, reconfigure it, and then drive it to work the next day.

Note that altering the system configuration during discharging is possible in theory, but in practice, we should only reconfigure the system when the load is disconnected and when proper safety protections are provided, leading to limited reconfiguration opportunities. This is because online system configuration causes safety risks such as arc flash due to voltage transients or loose connections, and the resultant inrush current could be as high as 50x of the normal current, jeopardizing system safety. Actually, a rule-of-thumb when reconfiguring electricity systems is to de-energize. This way, we do not consider such *reconfiguration-during-discharge* scenarios here.

The cell information during charging and discharging are logged, based on which their SoH are estimated and updated.[3] Our objective is to design SoH-aware reconfiguration algorithms to identify the proper system configuration based on cells' SoH, thus increasing the battery pack's capacity delivery.

E. Why SoH-Aware?

To show how SoH-aware reconfiguration improves battery pack performance, let us consider the example shown in Fig. 5(a) consisting of four cells with 2, 300mAh nominal capacity. Cell A and B are of 100% SoH and deliver a full capacity of 2, 300mAh upon fully charged, while cell C and D are of only 80% SoH, indicating a 1, 840mAh deliverable capacity with a single charge. Connecting these cells into the SoH-oblivious configuration $\overline{AC}||\overline{BD}$ as shown in Fig. 5(b),[4] only 1, 840mAh capacity can be delivered from each string, dominated by the weakest cells (i.e., cell C and D in their respective string). So, the SoH-oblivious configuration delivers only $1,840 \times 2 = 3,680$mAh capacity, and the remaining $2,300 - 1,840 = 460$mAh in cell A and B cannot be effectively utilized. On the other hand, if cells with similar SoH are organized to share the same string, i.e., the SoH-aware configuration $\overline{AB}||\overline{CD}$ (as in Fig. 5(c)), 2, 300mAh and 1, 840mAh capacity can be delivered by string $\overline{AB}$ and $\overline{CD}$, respectively, leading to 4, 140mAh total capacity delivery and about 12.5% increase when compared with Fig. 5(b).

[2]Note that the weight of vertices can be defined according to the problem tackled. For example, instead of the cells' SoH as in this work, $\mathcal{W}$ is defined as the real-time cell voltages in [6] to facilitate the matching between the supplied and the load required voltages.

[3]The estimation of cells' SoH is not the focus of this paper and will be explained in Section VII.

[4]In this notation, the overline indicates the series connection, and || represents the parallel connection.

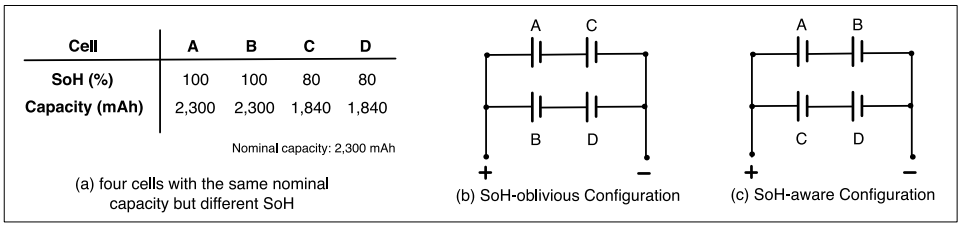

Fig. 5. Necessity of SoH-aware configuration.

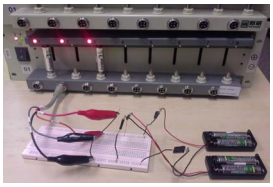

Fig. 6. Measurement settings with four rechargeable cells.

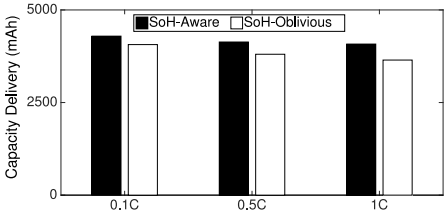

Fig. 7. Delivered capacities with different discharge currents.

Next we use the same 4 cells as in Fig. 2 to experimentally verify the above example. We fully charge the cells and connect them in the SoH-oblivious and SoH-aware configurations as shown in Fig. 5(b) and Fig. 5(c). The NEWARE battery tester is used to discharge these cells with currents of 0.1C, 0.5C, and 1C, respectively, as shown in Fig. 6. Fig. 7 plots the capacity delivery of the two configurations: SoH-aware delivers more capacity than the SoH-oblivious in all three cases, especially with larger discharge currents.

These results imply that only cells with similar SoH should be connected in series (and thus share the same string) to increase the battery pack's capacity delivery. We will introduce our design on SoH-aware reconfiguration in the next section.

IV. SoH-Aware Reconfiguration

A. On Fully Reconfigurable Packs

We first investigate the SoH-aware reconfiguration for fully reconfigurable battery packs, i.e., the cells in the battery pack can be arbitrarily connected. This, in practice, is the case when the battery pack can be removed from the load, and the cells therein can be reconfigured offline.

1) Problem Formulation: A fully reconfigurable battery pack can be captured by a fully connected graph, and any subset of cells in the pack can be connected in series. As a result, a total number of $m = \lfloor \frac{N}{n} \rfloor$ disjoint cell strings $\{s_1, s_2, \ldots, s_m\}$ can be formed. The challenge resides in how to construct such m strings to maximize the capacity delivery.

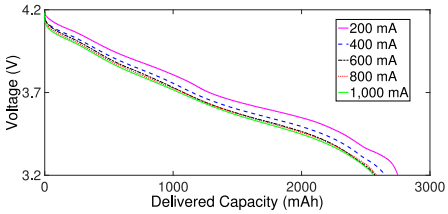

Fig. 8. Less capacity is delivered with larger discharge currents.

Note that the requirement on disjoint strings is to avoid including the same cell into multiple strings, in which case the discharge current of the shared cell would be larger than other non-shared cells. This is not desirable because of two reasons. First, the heterogeneous discharge currents among cells make the cell imbalance worse. Second, the larger discharge current of the shared cell degrades its capacity delivery because of the rate-capacity effect [6], i.e., cells' capacity delivery decreases with larger discharge currents. Fig. 8 plots our measurements on discharging a 2,900mAh Lithium-ion cell with different currents: the delivered capacity when discharging with 1,000mA current is 188mAh less than that delivered with a current of 200mA.

Without loss of generality, denote $H = \{h_1, h_2, \ldots, h_N\}$ as the estimated SoH for the N cells $\{b_1, b_2, \ldots, b_N\}$ in descending order, i.e., $\forall i < j \;\Rightarrow\; h_i \geq h_j$. Define an indicator variable $a_{i,j}$ as

$$a_{i,j} = \begin{cases} 1 & \text{if } b_i \in s_j \\ 0 & \text{otherwise.} \end{cases}$$

To capture the requirement on disjoint strings, we further define the conflict relationship between two strings s_i and s_j as

$$conflict(s_i, s_j) = 1 \Longleftrightarrow \exists k \in \{1, 2, \ldots, N\},\ a_{k,i} \cdot a_{k,j} = 1,$$

Because the string's deliverable capacity is dominated by the cell with the lowest SoH, the deliverable capacity C_j for string s_j can be captured by

$$C_j = \min\{a_{i,j} \cdot h_i\}^+ \cdot c \qquad (i = 1, 2, \ldots, N), \tag{2}$$

where $\min\{\cdot\}^+$ identifies the minimum non-zero value and c is the cell nominal capacity.

As a result, our problem to maximize the deliverable capacity can be formulated as

$$\max \sum_{j=1}^{m} C_j$$
$$s.t. \quad \forall i, j,\ x_i \cdot x_j = 1 \implies conflict(s_i, s_j) = 0. \tag{3}$$

2) SHARE-Full: We propose `SHARE-Full`, a simple but efficient solution to solve the above problem and prove its optimality in delivering the maximum capacity.

`SHARE-Full` forms the first string with the n cells with the highest SoH, and repeat the process with remaining cells until all the m strings have been formed. This way, we know $C_i = h_{(i\times n)}\cdot c$ and the totally deliverable capacity is $\sum_{i=1}^{m} C_i = \sum_{i=1}^{m} h_{(i\times n)}\cdot c$. Clearly, the time to sort cells according to their SoH dominates the computation complexity of `SHARE-Full`, which is $\mathcal{O}(\log N)$. Next we will show that although simple, `SHARE-Full` achieves an optimal capacity delivery.

Theorem 1: For battery packs with full reconfigurability, `SHARE-Full` identifies the configuration with the maximum deliverable capacity.

The above theorem can be proven by contradictory, which is not included here due to the space limit.

B. On Partially Reconfigurable Packs

In this section, we investigate the SoH-aware reconfiguration for battery packs with partial reconfigurability.

1) Problem Formulation: Unlike the case with fully reconfigurable battery packs where any n cells can be organized into a string, not any n cells can be connected in series when the battery pack offers only partial reconfigurability. This way, to identify the configuration with the maximum capacity delivery, the first step is to identify all possible n-cell strings in the battery pack.

With the graph representation of the battery pack, we can transform the problem of identifying the n-cell strings in the battery pack to finding the simple paths consisting of n vertices in the corresponding graph G. Although it can be shown that finding all n-vertex paths in G is NP-hard by deducing it from the longest path problem [22], an $\mathcal{O}(\Delta^{n-1}N^{2.37})$ algorithm has been proposed in [8], where Δ is the out-degree of vertices in G. For reconfigurable battery packs, the number of cells that a specific cell can connect to is limited due to the constraint on system complexity [6]. This is reflected in G that Δ will not be large, which significantly reduces the computation complexity to identify these paths. Furthermore, with a given battery pack, all the n-cell strings can be identified offline and stored in the battery management system, and then we only need to search through these pre-identified strings whenever the system reconfiguration is required.

Denote $\mathcal{P} = \{P_1, P_2, \ldots, P_M\}$ as the set of all n-vertex simple paths in the graph. Similar to the conflict relationship for two strings, the conflict relationship between two paths P_i and P_j is defined as

$$conflict\big(P_i, P_j\big) = 1 \Longleftrightarrow \exists k \in \{1, 2, \ldots, N\},\ a_{k,i}\cdot a_{k,j} = 1,$$

meaning that the two paths share certain common vertices (cells). Again, the conflicted paths should not be included in the final configuration, as explained in Section IV-A.

Denote x_i $(i = 1, 2, \ldots, M)$ as the indicator of whether P_i has been included in the final configuration

$$x_i = \begin{cases} 1 & \text{if } P_i \text{ is involved in the final configuration} \\ 0 & \text{otherwise.} \end{cases}$$

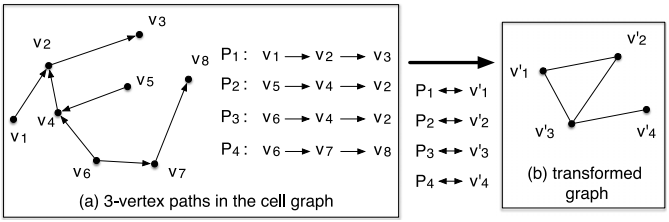

Fig. 9. Graph transformation.

The deliverable capacity C_i of path P_i can be calculated in the same way as in Eq. (2). Therefore, our problem in maximizing battery pack's capacity delivery is formulated as

$$\begin{aligned} \max\ \ & \mathcal{C} = \sum_{k=1}^{M} x_k \cdot C_k \\ s.t.\quad & \forall i, j,\quad x_i \cdot x_j = 1 \implies conflict\big(P_i, P_j\big) = 0. \end{aligned} \tag{4}$$

2) Problem Transformation: To shed more light on the above problem formulation, we first perform the following problem transformation, which not only help us to show its NP-hardness, but also inspires us the design of a simple but efficient solution.

With the path set $\mathcal{P}$ and their conflicting relationship, we can construct another graph G' by

- mapping each $P_i \in \mathcal{P}$ to a vertex v'_i in G';
- an edge connecting any two vertices v'_i and v'_j in G' exist if and only if the two paths corresponding to the two vertices in the original graph G conflict with each other (i.e., $conflict(P_i, P_j) = 1$); and
- the weight on vertex v'_i in G' is the deliverable capacity C_i of the corresponding path in G.

Fig. 9 shows an example on the graph transformation. Consider the case where 3-cell strings are required to support the load. After constructing the graph representation of an 8-cell battery pack, four 3-vertex paths are found as shown in Fig. 9(a). With the graph transformation operations, the four paths (i.e., P_1, P_2, P_3, P_4) are mapped to four vertices in G' (i.e., v'_1, v'_2, v'_3, v'_4). Furthermore, because P_1 and P_2 share a common vertex v_2 in G, the corresponding vertices v'_1 (for P_1) and v'_2 (for P_2) are connected by an edge in G'. The existence of other edges in G' can be explained similarly.

With the new graph G', our problem in (4) can be transformed to identify a subset of vertices in G' with the maximum weight sum, and the requirement on the disjoint paths in G can be captured by the requirement on the independent vertex pair in G'. As a result, the problem can be transformed to *finding a subset of vertices in G' such that 1) no edges exist between any pair of vertices in the subset, and 2) the weight sum of vertices in the subset is the largest*. Clearly, this is the maximum-weight independent set problem [22], which is known to be NP-hard. With any given instance of the maximum-weight independent set problem, we can deduce it to a special case of our problem by reversing the graph transformation, which proves the NP-Hardness of our problem.

3) SHARE-Partial: Although the maximum-weight independent set problem is known to be NP-hard, it has been

shown that the greedy solution for its non-weighted version achieves a solution with bounded optimality [23]. This inspires us the design of SHARE-Partial.

For each vertex v_i' in G', the gain to include it into the independent set is the amount of its deliverable capacity C_i. On the other hand, once adding v_i' into the configuration, all its directly neighboring vertices cannot be included anymore. In SHARE-Partial, we greedily add the vertex v_i' with the largest C_i to the dominating set until no vertices can be included any more, i.e., a maximal independent set is formed. At last, the selected vertices are transformed back to the paths in the original graph, and the configuration of the battery pack is identified.

Theorem 2: For battery packs with partial reconfigurability and in terms of maximizing their capacity delivery, SHARE-Partial achieves a performance ratio of

$$\frac{\left(\Delta'+2\right)\cdot C_{\max}}{3\cdot C_{\min}}, \tag{5}$$

when compared with the optimal solution, where $C_{\max}$ and $C_{\min}$ are the largest and smallest deliverable capacity of all the n-cell strings, and Δ' is the maximal degree of vertices in the transformed graph G'.

It has been proved in [23] that a performance ratio of $\frac{\Delta+2}{3}$ can be achieved by the greedy solution for the maximum independent set problem (i.e., when vertices have uniform weight). The above theorem can be proved by incorporating the vertices weight into the proof therein.

V. Performance Analysis

We analytically explore the capacity delivery with SHARE-Full in this section, and compare it with the non-reconfigurable case. This analysis on SHARE-Full also serves an upper bound for the capacity delivery with SHARE-Partial.

A. Capacity Delivery With SHARE-Full

Conventional wisdom says the cell imbalance can be captured by normal distributions [16]. Denoting h as cells' SoH

$$h\sim\mathcal{N}\left(\mu,\sigma^2\right), \tag{6}$$

and define h_i $(i=1,2,\ldots,N)$ as the SoH of the ith strongest cell in the battery pack. With SHARE-Full, the strongest n cells form the first string, whose capacity delivery is dominated by the nth strongest one — the cell with SoH h_n. The CDF of h_n can be derived as

$$P\{h_n<x\}=\sum_{k=0}^{n-1}\binom{N}{k}(1-P\{h\le x\})^k P\{h\le x\}^{N-k}.$$

This way, the capacity delivery of this strongest string, C_1, can be derived as

$$F_{str}^1(x)=P\{C_1<x\}=P\{h_n<x/c\}, \tag{7}$$

and $f_{str}^1(x)=\frac{\partial F_{str}^1(x)}{\partial x}$. The CDFs of the capacity delivery of other strings can be calculated similarly.

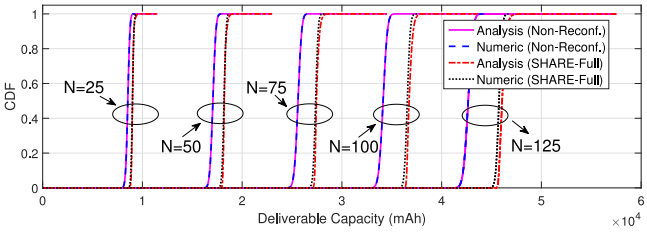

Fig. 10. Distribution of battery packs' capacity delivery.

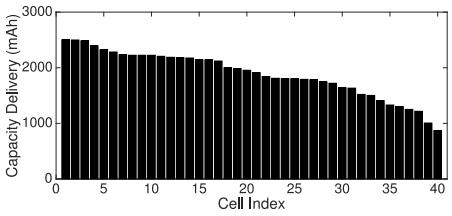

Fig. 11. Capacity of 40 cells.

TABLE I
Default Settings in Numerical Evalutions

μ	σ	n	m	N	c
0.8	0.05	5	5–25	25–125	2, 300mAh

The total capacity delivery of the battery pack can be approximated based on the convolution theorem as

$$C_{\text{SHARE-Full}}\sim f_{str}^1(x)*f_{str}^2(x)*\cdots*f_{str}^m(x), \tag{8}$$

where $*$ denotes the convolution operation.[5]

B. Capacity Delivery With Non-Reconfigurable Packs

Next let us consider the capacity delivery of non-reconfigurable battery packs. In this case, the capacity delivery of each string is dominated by the weakest cell among n cells, whose SoH conforms to

$$P\{h_{weakest}<x\}=1-(1-P\{h\le x\})^n, \tag{9}$$

and thus the capacity delivery of the strings follows

$$\begin{aligned}F_{str}(x)&=P\{C_{str}<x\}=P\{c\cdot h_{weakest}<x\}\\&=P\{h_{weakest}<x/c\}.\end{aligned} \tag{10}$$

Again, $f_{str}(x)=\frac{\partial F_{str}(x)}{\partial x}$.

This way, we know the overall capacity delivery for non-reconfigurable battery packs conforms to

$$C_{\text{Non-Reconf}}\sim f_{str}^{(m)}(x), \tag{11}$$

where $f_{str}^{(m)}(x)$ denotes the m-fold convolution of $f_{str}(x)$.

C. Numerical Validation

The above results allow us to analytically explore the advantage of SHARE-Full. Numerical evaluations are performed to verify their accuracy. The default settings in these numerical evaluation are summarized in Table I. Fig. 10 plots the CDFs

[5]Here we use the term *approximated* because the independency among C_is is required by the convolution theorem. The accuracy of this approximation is validated with our numerical results as will be shown later.

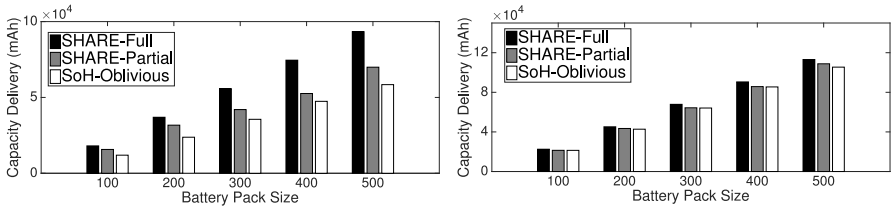

(a) based on all cells in Fig. 11. **(b)** based on only cells with SoH >80%

Fig. 12. Capacity delivery w.r.t battery pack size.

of the capacity delivery of battery packs with varying scales, which demonstrates *(i)* the accuracy of the above analysis, and *(ii)* the advantage of `SHARE-Full` is pronounced with larger battery pack scales.

VI. Evaluations

We have evaluated our design both via emulations and experimentally.

A. Trace-Driven Emulations

We first evaluate `SHARE-Full` and `SHARE-Partial` via emulations based on empirically collected discharged traces of 40 Li-ion cells, whose capacity delivery is summarized in Fig. 11. Then we emulate fully-, partially-, and non-reconfigurable battery packs with these cells, i.e., each cell in the packs are randomly emulated to be one of the cells in Fig. 11.

Fig. 12(a) compares the capacity delivery of the emulated battery packs with different sizes, with a load required string size of 10. As expected, more capacity is delivered with `SHARE-Full`, especially with larger battery packs. For example, when compared with the SoH-oblivious case, a 51% increase in capacity delivery can be obtained with a 100-cell battery pack, which further increases to 60% for 500-cell packs. These observations show the necessity of SoH-aware configuration especially for large battery systems. `SHARE-Partial` delivers less capacity when compared to the fully-reconfigurable case, which is intuitive due to reduced reconfigurability. However, it still improves the capacity delivery when compared with the SoH-Oblivious case by 15–33%. Limiting the SoH range by selecting only cells of SoH larger than 80%, Fig. 12(b) plots the capacity delivery for thus-emulated battery packs. The improvement in capacity delivery, albeit not any significant as in Fig. 12(a) due to less cell imbalance, can still be clearly observed.

B. Experiment-A

We also use two experiments to evaluate `SHARE-Full` and `SHARE-Partial`. We introduce our first set of experiments in the next.

• **Cells and their SoH.** We form a 15-cell battery pack with 2, 300mAh rechargeable cells. We fully charge these cells with their associated commercial chargers, then we discharge them individually with 1C rate and record their delivered capacity, based on which their SoH is estimated as shown in Table II. Fig. 13(a) shows the laboratory settings for the experiments.

TABLE II
SoH of Cells Used in Experiment-A

Cell	#1	#2	#3	#4	#5
Cap. (mAh)	1781.7	2188.0	2224.5	1841.4	1721.2
SoH (%)	77.5	95.1	96.7	80.1	74.8
Cell	**#6**	**#7**	**#8**	**#9**	**#10**
Cap. (mAh)	2224.5	1911.2	2224.2	1802.2	2139.5
SoH (%)	96.7	83.1	96.7	78.4	93.0
Cell	**#11**	**#12**	**#13**	**#14**	**#15**
Cap. (mAh)	2291.4	1791.6	1805.0	2205.7	2142.2
SoH (%)	99.6	77.9	78.5	95.9	93.1

• **Loads.** In the experiment, we consider the case where 3-cell strings are required to support the load, which demands a discharge current of 2, 300mA. Again, the NEWARE battery testing system is used to control the discharge current.

• **Battery Packs.** We emulate three battery packs with different reconfigurability:

- a *non-reconfigurable battery pack*, where five 3-cell strings are formed by cells $\{\overline{1, 2, 3}\}$, $\{\overline{4, 5, 6}\}$, $\{\overline{7, 8, 9}\}$, $\{\overline{10, 11, 12}\}$, and $\{\overline{13, 14, 15}\}$, respectively. In other words, the cells are connected sequentially according to their indexes without considering their SoH.
- a *partially reconfigurable battery pack*, which is constructed on top of the sequential configuration by allowing each cell to connect to another random cell: the ith cell in the pack can be directly connect to (i) the $i+1$th cell and (ii) another random cell besides i and $i+1$.
- a fully reconfigurable battery pack, where any subset of cells can be connected in series.

Applying `SHARE-Full` and `SHARE-Partial` to the fully and partially reconfigurable battery packs, respectively, the identified SoH-aware configurations are:

$$\text{Fully:}\overline{\{11, 6, 8\}}||\overline{\{3, 14, 2\}}||\overline{\{15, 10, 7\}}||\overline{\{4, 13, 9\}}||\overline{\{12, 1, 5\}},$$
$$\text{Partially:}\overline{\{7, 8, 15\}}||\overline{\{9, 10, 11\}}||\overline{\{2, 13, 14\}}||\overline{\{3, 4, 5\}}||\overline{\{1, 6, 12\}}.$$

Then we connect the cells according to the obtained configurations to power the loads, and the discharging process terminates when the pack' output voltage reduces to 1.5 V.

• **Methodologies:** Our experiments consist of two parts as illustrated in Fig. 13(b). First, the fully charged battery packs are directly connected to the load, which assists to reveal the fundamental impact of the SoH-aware configuration on the battery packs' deliverable capacity. Second, an LM 1117 voltage regulator and a protection diode is inserted between each of the 3-cell string and the load, as in most practical applications with parallel connected strings. This experiment setting

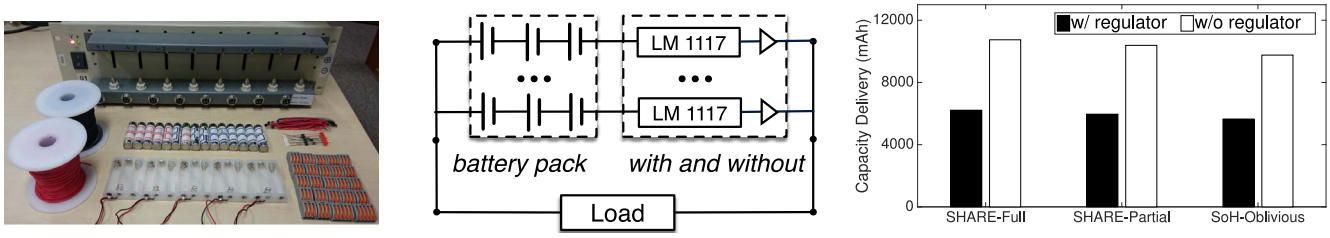

(a) Lab settings for Experiment-A **(b)** Methodology **(c)** Results

Fig. 13. Experiment evaluation of SHARE-Full and SHARE-Partial.

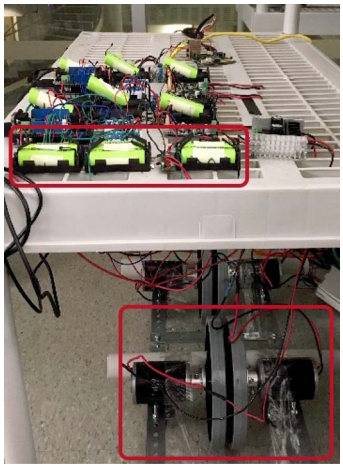

Fig. 14. Lab settings for Experiment-B.

TABLE III
SOH OF CELLS USED IN EXPERIMENT-B

Cell	#1	#2	#3	#4	#5	#6
SoH (%)	73	93	85	83	92	90

TABLE IV
CAPACITY DELIVERY IN EXPERIMENT-B (MAH)

	1st Run	2nd Run	3rd Run	4th Run
SHARE-Full	3,204	3,128	3,189	3,228
SoH-Oblivious	2,898	2,786	2,803	2,923

reveals the practical effect of the SoH-aware configuration in enhancing the capacity delivery.

The experiment results are summarized in Fig. 13(c). Taking the SoH-oblivious configuration as the baseline, when directly connecting the battery packs with the load, 10.1% and 6.5% more capacity can be delivered with the fully and partially reconfigurable battery packs. These improvement ratios are 10% and 5.5%, respectively, when voltage regulators and diodes are used in the experiments. Further comparing the two experiment settings (i.e., w/ and w/o regulators), we can see that the capacity delivery is largely reduced when the regulators and the protection diodes are adopted. This is because these complimentary components introduces non-negligible energy loss, thus reducing the capacity that can be drawn to power the loads.

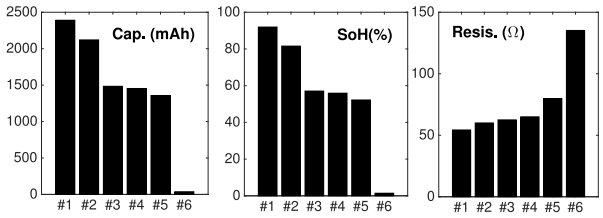

Fig. 15. Capacity delivery, SoH, and internal resistance of 6 ICR18650 Lithium-ion cells, showing strong negative correlation.

C. Experiment-B

In the second experiments, we emulate fully- and non-reconfigurable battery packs with 6 Li-ion cells, whose SoH is listed in Table III. These cells are fully charged with $<0.5C, 4.2V, 0.05C>_{\text{cccv}}$, connected in 3S2P, and then discharged by a 12V motor. The experiment is logged at 100Hz and stops when any cell's voltage reduces to the cut-off level of 3.0V. Fig. 14 shows the experiment settings. The cells are connected sequentially in the non-reconfigurable battery pack, and their connectivity determined after applying `SHARE-Full` to the fully reconfigurable pack is $\overline{\{1,3,4\}}||\overline{\{2,5,6\}}$. The experiments are run 4 times for each battery packs and thus-collected capacity deliveries are summarized in Table IV: `SHARE-Full` delivers 300–400mAh more capacity when compared with the non-reconfigurable case.

Failure of cells occurs in practice and leads to severe cell imbalance. We emulate the case that cell-6 fails in the pack, making the corresponding string open. This way, cells are connected as $\overline{\{1,2,3\}}||\overline{\{4,5,\mathsf{X}\}}$ in the non-reconfigurable pack, and as $\overline{\{2,3,5\}}||\overline{\{1,4,\mathsf{X}\}}$ after applying `SHARE-Full` to the fully reconfigurable one, treating the SoH of cell-6 as 0. The experiments show that 1,045mAh capacity is delivered with the non-reconfigurable pack, and that with `SHARE-Full` is 1,626mAh: a 55.58% improvement.

VII. PRACTICAL ISSUE ON SOH ESTIMATION

SoH estimation of cells is supported by many off-the-shelf battery management systems/chips [20], which can be achieved based on different system parameters such as internal resistance, number of life cycles, etc. Next we briefly explain two classic SoH estimation methods.

The first approach of SoH estimation is to test cells' capability to accept/delivery charge, as used in the battery management chip of MAX17047. Fully charging and then

discharging cells with a small current, their SoHs can be estimated as the ratios between the discharged capacity and their nominal capacity [17], e.g., if 2, 000 mAh capacity is delivered when discharging a cell rated at 2, 450 mAh, it indicates the cell has a SoH of $\frac{2,000}{2,450} = 81.6\%$.

Cells' SoHs can also be inferred from their internal resistance. To verify the correlation between cells' SoH and their resistance, we collect 6 Li-ion cells, measure their capacity delivery upon fully charge (with the specified charging profile in their data sheet), estimate their SoH based on the capacity delivery, and compare these information with their resistance measured by a BVIR meter. Fig. 15 summaries the measurement results, showing the cells' SoH is strongly and negatively correlated with their resistance with a -0.94 correlation coefficient. This allows to determine cells' SoH by checking a look-up table identified offline [24].

VIII. Conclusion

In this paper, we mitigate cell imbalance via SoH-aware reconfiguration in battery packs, which jointly explores the system reconfigurability and the state-of-health of cells to enhance the capacity delivery of battery packs. We propose two SoH-aware configuration algorithms, `SHARE-Full` and `SHARE-Partial`, focusing on fully and partially reconfigurable battery packs, respectively. We evaluate `SHARE-Full` and `SHARE-Partial` using both experiments and emulations, showing a 10–60% improvement of battery pack's capacity delivery especially with severe cell imbalance.

References

[1] L. He, Y. Gu, C. Liu, T. Zhu, and K. G. Shin, "SHARE: SoH-aware reconfiguration to enhance deliverable capacity of large-scale battery packs," in *Proc. ICCPS*, Seattle, WA, USA, 2015, pp. 169–178.

[2] S. Ci, J. Zhang, H. Sharif, and M. Alahmad, "Dynamic reconfigurable multi-cell battery: A novel approach to improve battery performance," in *Proc. APEC*, Orlando, FL, USA, 2012, pp. 439–442.

[3] T. Kim, W. Qiao, and L. Qu, "A series-connected self-reconfigurable multicell battery capable of safe and effective charging/discharging and balancing operations," in *Proc. APEC*, Orlando, FL, USA, 2012, pp. 2259–2264.

[4] S. Ci, N. Lin, and D. Wu, "Reconfigurable battery techniques and systems: A survey," *IEEE Access*, vol. 4, pp. 1175–1189, 2016.

[5] H. Kim and K. G. Shin, "On dynamic reconfiguration of a large-scale battery system," in *Proc. RTAS*, San Francisco, CA, USA, 2009, pp. 87–96.

[6] L. He, L. Gu, L. Kong, Y. Gu, C. Liu, and T. He, "Exploring adaptive reconfiguration to optimize energy efficiency in large-scale battery systems," in *Proc. RTSS*, Vancouver, BC, Canada, 2013, pp. 118–127.

[7] Y. Kim *et al.*, "Balanced reconfiguration of storage banks in a hybrid electrical energy storage system," in *Proc. ICCAD*, San Jose, CA, USA, 2011, pp. 624–631.

[8] L. He *et al.*, "Reconfiguration-assisted charging in large-scale lithium-ion battery systems," in *Proc. ICCPS*, Berlin, Germany, 2014, pp. 60–71.

[9] F. Jin and K. G. Shin, "Pack sizing and reconfiguration for management of large-scale batteries," in *Proc. ICCPS*, Beijing, China, 2012, pp. 138–147.

[10] A. Badam *et al.*, "Software defined batteries," in *Proc. SOSP*, Monterey, CA, USA, 2015, pp. 215–229.

[11] T. Kim, W. Qiao, and L. Qu, "Power electronics-enabled self-X multicell batteries: A design toward smart batteries," *IEEE Trans. Power Electron.*, vol. 27, no. 11, pp. 4723–4733, Nov. 2012.

[12] S. Ci, J. Zhang, H. Sharif, and M. Alahmadu, "A novel design of adaptive reconfigurable multicell battery for power-aware embedded networked sensing systems," in *Proc. GLOBECOM*, 2007, pp. 1043–1047.

[13] H. Kim and K. G. Shin, "Dependable, efficient, scalable architecture for management of large-scale batteries," in *Proc. ICCPS*, Stockholm, Sweden, 2010, pp. 178–187.

[14] T. Kim, W. Qiao, and L. Qu, "Series-connected self-reconfigurable multicell battery," in *Proc. APEC*, Fort Worth, TX, USA, 2011, pp. 1382–1387.

[15] B. A. M. Molenaar, "Reconfigurable battery system for ultra fast charging of industrial electric vehicles," M.S. thesis, Dept. Elect. Eng., Delft Univ. Technol., Delft, The Netherlands, 2010.

[16] L. H. Goldberg. (2011). *Battery Cell Balancing for Improved Performance in EVs*. [Online]. Available: https://www.digikey.com/en/articles/techzone/2011/oct/battery-cell-balancing-for-improved-performance-in-evs—part-i-passive-balancing-technologies

[17] G. L. Plett, "Recursive approximate weighted total least squares estimation of battery cell total capacity," *J. Power Sources*, vol. 196, no. 4, pp. 2319–2331, 2011. [Online]. Available: http://www.sciencedirect.com/science/article/pii/S037877531001654X

[18] D. Andrea, *Battery Management Systems for Large Lithium-Ion Battery Packs*. Boston, MA, USA: Artech House, 2010.

[19] J. L. Vian, A. R. Mansouri, R. Elangovan, M. M. Borumand, and K. Abdel-Motagaly, "Health management of rechargeable batteries," U.S. Patent, 20 100 121 587, 2010.

[20] S. J. Moura, J. L. Stein, and H. K. Fathy, "Battery-health conscious power management in plug-in hybrid electric vehicles via electrochemical modeling and stochastic control," *IEEE Trans. Control Syst. Technol.*, vol. 21, no. 3, pp. 679–694, May 2013.

[21] S. Zeljkovic, T. Reiter, and D. Gerling, "Efficiency optimized single-stage reconfigurable DC/DC converter for hybrid and electric vehicles," *IEEE J. Emerg. Sel. Topics Power Electron.*, vol. 2, no. 3, pp. 496–506, Sep. 2014.

[22] R. Diestel, *Graph Theory*, 3rd ed. New York, NY, USA: Springer, 2005.

[23] M. M. Halldórsson and J. Radhakrishnan, "Greed is good: Approximating independent sets in sparse and bounded-degree graphs," *Algorithmica*, vol. 18, no. 1, pp. 145–163, 1997.

[24] S. Analytical, *Accurate Estimates of Critical Battery Parameters Using Electrochemical Impedance Spectroscopy*, AZO Mater., Manchester, U.K., 2016.

Authors' photographs and biographies not available at the time of publication.